



A New Approach to Robust LiDAR/Optical Imagery Registration

HUI JU, CHARLES TOTH & DOROTA A. GREJNER-BRZEZINSKA, Columbus, Ohio, USA

Keywords: LiDAR intensity image, aerial/satellite image, registration, LPFFT, MI, SIFT

Summary: Most of the image registration/matching methods are applicable to images acquired by either identical or similar sensors from various positions. Simpler techniques assume some object space relationship between sensor orientations, such as near parallel image planes, certain overlap, and comparable radiometric characteristics. More robust high-level feature-based methods allow for larger variations in image orientation and texture; for example, SIFT (scale invariant feature transform), a highly robust registration technique for wide baseline images. Nevertheless, registration between LiDAR (light detection and ranging) intensity and optical (satellite and aerial) images is still a big challenge, as substantial differences do exist in their radiometric characteristics. Reviewing and testing popular multiple domain image registration techniques, such as feature-based SIFT, intensity-based MI (mutual information), and frequency-based LPFFT (log-polar fast fourier transform), it is realized that no single technique could solve LiDAR intensity and optical image registration completely. Alternatively, a new approach to robust LiDAR/optical imagery registration, taking advantages of feature-, intensity-, and frequency-based methods, is proposed. Initial testing with a few datasets showed good performance of the new method, achieving pixel-level accuracy for the registration.

Zusammenfassung: Die meisten Methoden der Bildregistrierung/Bildanpassung können auf Bilder angewandt werden, die entweder mit identischen oder ähnlichen Sensoren aus verschiedenen Positionen aufgenommen werden. Einfachere Techniken basieren auf der Annahme eines speziellen Zusammenhangs im Objektraum, wie z.B. annähernd parallele Bildebenen, eine bestimmte Überlappung oder ähnliche radiometrischen Eigenschaften. Robustere high-level merkmalsbasierte Methoden ermöglichen größere Variationen in Bildorientierung und -textur, z.B. SIFT (Scale Invariant Feature Transform), eine sehr robuste Technik für die gegenseitige Registrierung von Bildpaaren mit langen Basislinien. Dennoch ist die Registrierung von LiDAR (Light Detection And Ranging) Intensitätsbildern und optischen (satelliten- oder flugzeuggestützten) Bildern noch immer eine große Herausforderung, da erhebliche Unterschiede in ihren radiometrischen Eigenschaften bestehen. Ein Test mehrerer beliebter Techniken zur Registrierung von Bildern aus unterschiedlichen Domänen wie z.B. das merkmalsbasierte Verfahren auf Basis von SIFT, das intensitätsbasierte Verfahren mit Hilfe von MI (Mutual Information) sowie das frequenzbasierte Verfahren LPFFT (Log-Polar Fast Fourier Transform), haben gezeigt, dass keine Technik einzeln das Problem der Registrierung von LiDAR Intensitätsbildern und optischen Bildern vollständig lösen kann. Als Alternative wird eine neue Bildregistrierungsmethode für LiDAR Intensitäts- und optische Bilder vorgeschlagen, welche die Vorteile der merkmalsbasierten, intensitätsbasierten und frequenzbasierten Methoden verbindet. Erste Tests des Verfahrens mit wenigen Datensätzen lieferten gute Ergebnisse mit Genauigkeiten in der Größenordnung von einem Pixel.

1 Introduction

1.1 Motivation

Image registration is a core task for various applications in digital photogrammetry, computer vision, remote sensing, and vision-aided navigation. Its purpose is to estimate the geometric transformation using an adequate number of correspondences between images acquired at different times, perspectives or even from different sensors. Image matching methods, computing those correspondences, are typically applicable to images acquired by either identical or similar sensors from various positions, and in the past few years, much effort has been devoted to develop automatic tie point extraction methods (REMONDINO & RESSL 2006).

As a growing number of various image sensors provide multiple image coverage worldwide, the need for registering imagery acquired from different airborne and spaceborne platforms is growing. Several satellite systems deliver high resolution imagery in short repeat time, large-format aerial digital cameras provide multispectral imagery at unprecedented resolution, LiDAR (light detection and ranging) systems collect both range and intensity images at local scale, while IfSAR (interferometric synthetic aperture radar) data are acquired from spaceborne and airborne platform at global scale, etc. All those data should be accurately registered for data fusion to support better geospatial data and information extraction.

The motivation for this study comes from three applications: terrain-based navigation, improving the geo-referencing of satellite imagery by using ground control, and developing a new man-made object modelling methods via fusing LiDAR and aerial images. In all those applications, LiDAR intensity and optical image registration plays an important role. It should be noted that data collected only from airborne/spaceborne platforms is considered in this study.

Registering LiDAR intensity and optical images is a particularly difficult task due to their substantially different characteristics, such as different sensing methodology (e.g.

wavelength, passive/active image acquisition), geometric and radiometric differences, etc. In a LiDAR system, electromagnetic pulses in the visible and/or infrared bands are emitted from a transmitter, and besides the range measurement, the strength of the reflected pulse is recorded, which is known as the intensity value. A LiDAR intensity image is typically generated by rasterizing the intensity values of the point cloud. With increasing laser point density, e.g. 8–15 points per m², it is possible to obtain high-resolution LiDAR intensity images; nevertheless, they are still poor in quality in comparison with optical images. The main reason is the problem of rasterizing the irregularly distributed point cloud. After several rasterization tests, 1 m GSD is selected based on our data.

1.2 Review of Multiple-Domain Image Registration Methods

Multiple-domain image registration, also known as multi-modal image registration, has been investigated for decades, and, in general, can be classified into three major categories: feature-based, intensity-based, and frequency-based.

Feature-based registration methods use the similarity between features from the image pair to determine the transformation parameters. Low-level feature-based techniques use low-level features, such as points, corners and edges extracted from images. Unfortunately, the identification of conjugate corners or edges is difficult in the LiDAR intensity and optical image pair due to the irregular and sparse nature of LiDAR points at break lines. High-level feature-based techniques use high-level features such as regional descriptors and shape descriptors. SIFT (LOWE 1999, 2004) can be regarded as a complex descriptor, which could provide good registration results between aerial and satellite images, but failed in LiDAR intensity and optical image domains (JU et al. 2011, TOTTH et al. 2010). The reason is that the substantial differences between the LiDAR intensity and optical image make the key points quite different in the two domains. Even for those key points extracted from similar loca-

tions, their descriptors can be still quite different, leading to mismatches. In contrast, fusing LiDAR and optical imagery for modelling of building facades is different. More importantly, the terrestrial laser scanner is much closer to the building, which can provide much denser and nearly regularly distributed points on the facades. Consequently, features, like corners of windows and doors, are easy to identify on the facades. Therefore, SIFT works rather well for terrestrial laser scanner and optical camera data (BÖHM & BECKER 2007, BECKER & HAALA 2008). For the airborne data, alternatively, other primitives, such as 3D straight lines and surface patches extracted from LiDAR data, are generally considered to be used to fuse optical images (HABIB et al. 2004, KIM & HABIB 2009). Note that in those approaches, LiDAR intensity is hardly considered.

Intensity-based registration methods usually define an intensity-based similarity measure between the templates (reference/target) or images, and then perform an optimization over allowed transformations to maximize this measure. For example, LSTM (least square template matching) is used to estimate the template-to-template transformation, which is normally an affine model (GRÜN 1985). Once enough correspondences are found via LSTM, the transformation between the image pair can be determined, and thus, image registration is achieved. For the multiple domain image registration, the method based on MI (mutual information) (VIOLA & WELLS 1997) is one of the most popular ones, widely used in medical imaging applications and proved to be very effective. The basic concept of MI-based image registration comes from the information theory. Each image is regarded as a 2D discrete signal, carrying information. If two images are matched, their mutual information should be large and their joint entropy should be small. The transformation parameters are solved via maximizing the MI value based target function, in which different kinds of constraints to describe feature characteristics or spatial information can be introduced to improve the registration results. Although a few studies applying MI-based registration methods on multiple domain imagery in the fields of photogrammetry and remote sensing are reported, such as registration between

TerraSAR-X and IKONOS images (SURI & REINARTZ 2010) as well as between terrestrial camera image and infrared image (LIU et al. 2010), they have not been applied to LiDAR intensity and optical images. According to our limited datasets, NMI (normalized mutual information) can be used to find the transformation parameters, in the latter case; preliminary test results are discussed in the section 2.2.

Frequency-based registration methods use characteristics, such as the phase in the spectral domain to determine the transformation parameters between two images. Note that these techniques are typically restricted to handle images with limited surface-induced distortions. A popular frequency-based method is LPFFT (log-polar fast fourier transform) which estimates the shift or similarity transformation between image pairs without any feature detection (REDDY & CHATTERJI 1996, WOLBERG & ZOKAI 2000, ZOKAI & WOLBERG 2005). Based on our experiences, it is difficult to achieve reliable results applying the traditional LPFFT to our data.

Experimental results of using SIFT, MI and LPFFT on LiDAR intensity and optical images are given in section 2.

1.3 Proposed Method

The main contribution of this paper is to propose a hybrid multiple domain image registration method using a coarse-to-fine strategy, which largely refines our previous approach (TOTH et al. 2011). First, a modified LPFFT with an internal validation module is used to estimate the coarse similarity transformation between LiDAR intensity and optical image pair. Next, strong HCs (Harris corners) in both images are generated and transformed to the other image via the estimated coarse transformation, and, subsequently, scale- and rotation-invariant PDF (probability density function) mean-shift matching (COMANICIU et al. 2003) is performed to find the correct correspondences. Finally, the RANSAC (random sample consensus) (FISCHLER & BOLLES 1981) scheme is used to remove outliers and estimate the parameters of an affine transformation.

1.4 Data

To support this study, two datasets were used. The 1 m GSD orthorectified satellite images by GeoEye, acquired in January 2010, and 1 m GSD intensity images from airborne LiDAR data by Fugro-EarthData from 2009 covering the San Diego, California, USA area, represent a typical mix of terrain topography and landscape, including residential areas, roads, and vegetated areas. The 0.2 m GSD high resolution DMC aerial imagery and 1 m GSD intensity image from LiDAR data by ODOT (the Ohio Department of Transportation) cover the corridor area of highway I-70 in the Belmont County and highway 161 in Franklin County, Ohio, USA.

2 Experiences with SIFT, MI and LPFFT

In this section, test results of applying SIFT, MI and LPFFT to LiDAR intensity and optical image registration are discussed. These experiences directly inspired us to seek an alternative approach.

2.1 SIFT

In our early study, the baseline SIFT implementation was used for multiple domain image registration. It was found that SIFT can provide reliable matching results between satellite and aerial images. However, based on our limited data, SIFT matching between LiDAR intensity and optical images is not reliable. Fig. 1 shows typical SIFT matching results for a LiDAR intensity and satellite image pair. The number of the matched features is pretty small, and, more importantly, none of the matches is correct for this image pair, though there are keypoints extracted at similar locations. The main reason for the failure of SIFT matching is that it is very difficult to find similar keypoints in both images due to the substantial differences in radiometric characteristics and, in some extent, spatial resolution.

2.2 MI

To assess the MI-based registration performance on LiDAR intensity and optical image pairs, only simplified test scenarios are used.

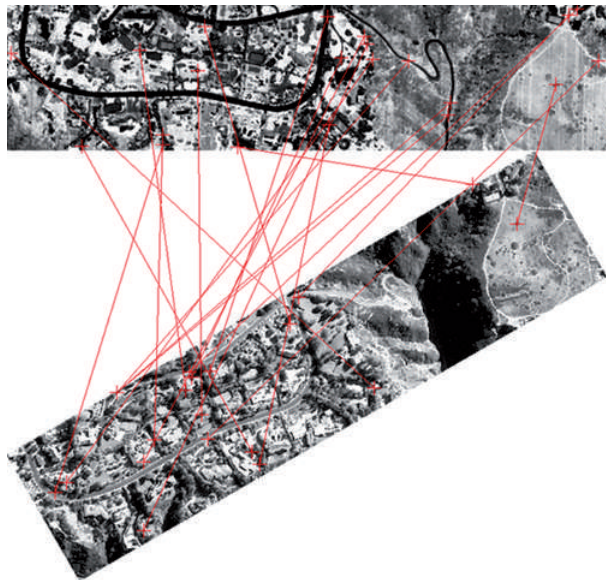


Fig. 1: SIFT matching results between LiDAR intensity image (top) and satellite image (bottom).

Also, the LiDAR intensity image is manually aligned with the optical image. Then, different scale, rotation and translation parameters are computed through expanding the correct parameters $(s_0, \varphi_0, t_{x0}, t_{y0})$ by a combination of incremental values $(\Delta s, \Delta\varphi$ and $\Delta t)$ via (1). Those parameters are applied to the optical image, and then, the NMI (normalized mutual information) is computed for each image pair. 3D surfaces extended by (s, φ, NMI) and (t_x, t_y, NMI) are used to visualize the performance. The NMI surface should peak at the location of the correct parameters (s_0, φ_0) and (t_{x0}, t_{y0}) , respectively. For our tests, $\Delta s = 0.05$, $\Delta\varphi = 1^\circ$ and $\Delta t = 1$ pixel. Fig. 2 illustrates the typical NMI surface w.r.t. translation parameters (a) and w.r.t. scale and rotation parameters (b). Clearly, NMI can be used to locate the correct parameters in a given searching space. Fig. 2b shows that NMI is more sensitive to scale than

to rotation angle, though, the correct scale and rotation parameters can be identified in the search space, see Fig. 3.

$$\begin{aligned}
 s &:= \{s | s_i = s_0 \pm i \Delta s\} \\
 \varphi &:= \{\varphi | \varphi_i = \varphi_0 \pm i \Delta\varphi\} \\
 t_x &:= \{t_x | t_{x0} \pm i \Delta t\}, t_y := \{t_y | t_{y0} \pm i \Delta t\}
 \end{aligned}
 \tag{1}$$

NMI is a reliable indicator to locate the correct transformation parameters in a given (limited) search space; however, the determination of the right search space can be difficult.

2.3 LPFFT

Using the LPFFT registration method, scale and rotation parameters of the similarity model are estimated in the first step. Next, the sec-

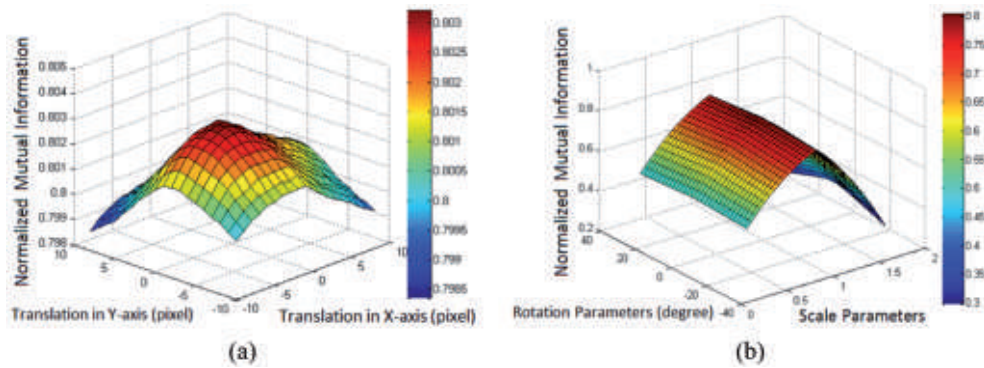


Fig. 2: (a) NMI surface expanded by translation parameters and (b) NMI surface expanded by rotation and scale parameters.

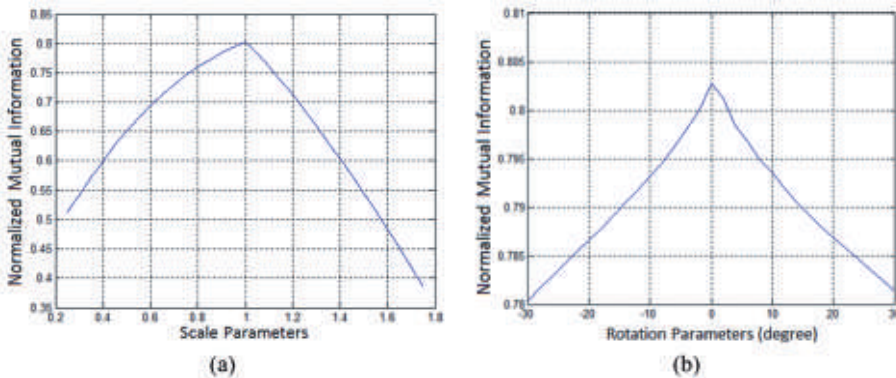


Fig. 3: (a) plot of NMI versus scale parameters and (b) plot of NMI versus rotation parameters.

ond image is transformed based on the estimated scale and rotation values, so the images have comparable orientation and scale. Finally, the translation parameters are estimated by NCC (normalized cross correlation). For efficient processing, FFT-accelerated NCC (FFT NCC) is used. In our testing, the cross phase correlation, i.e. the response to iFFT (inverse fast fourier transform) of the phase difference turned out to be very noisy. Simply considering the maximum response, which would indicate the correct scale and rotation parameters, is just not reliable. Therefore, a validation of the scale and rotation based on a Monte Carlo test is proposed, and provided good results.

According to our tests, using FFT NCC to compute the translation parameters is generally not reliable. Therefore, to estimate the translation parameters, a different approach was proposed. First, both images are converted into binary edge images; and then, a number of reference patches are automatically generated in the reference image. Next, the reference patches are matched in the second image based on template NCC matching. Ideally, image coordinate differences between all reference and matched patches should be identical, representing the common shift between the image pair. Our results confirmed the feasibility of the proposed procedure.

3 Methodology

Based on our experiences, the registration of the LiDAR intensity and optical image pair by the tested registration methods alone is just not reliable. Therefore, the coarse-to-fine hy-

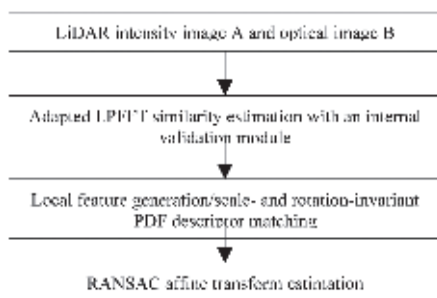


Fig. 4: Proposed multiple domain image registration workflow.

brid multiple domain image registration approach is proposed; the workflow is illustrated in the Fig. 4. In the following subsections, the main components will be discussed in detail.

3.1 Similarity Transformation Estimation

The workflow of the adapted LPFFT similarity estimation approach is given in the Fig. 5. First, using the LPFFT, two parameters (scale and rotation) of the similarity model are estimated. LPFFT could provide a number of possible scale and rotation parameters from which the correct ones have to be identified through a validation. The validation of the scale and rotation parameters is achieved via a Monte Carlo test; more specifically, a Monte Carlo test is performed for a set of scale and rotation values computed using (1), where the two originally estimated parameters (s_0 , ϕ_0) are perturbed by a combination of increment values (Δs , $\Delta\phi$). Next, the second image is transformed using each scale and rotation combination in the set. If the scale and rotation parameters are correct, the image pair should have comparable orientation and scale. FFT-accelerated NCC, an efficient NCC computation method, is used to estimate the translation parameters for each image pair based on the maximum NCC values. For correct scale and rotation parameters, the maximum NCC values of all image pairs should fall in a significantly high range, which means that small scale and rotation changes around the correct scale and rotation still lead to a high NCC value. If the estimated scale and rotation are wrong, the maximum NCC values of all image pairs should be small. Fig. 6 shows a typical NCC surface based on wrong and correct parameters, (s_0 , ϕ_0), respectively.

Next, the second image, B, is transformed using the estimated (correct) scale and rotation parameters, at which translation difference may still exist between the two images. To estimate the translation parameters, both images are converted into binary edge images. Then, a number of reference patches are automatically generated in the reference image, and finally, those reference patches are matched in the second image based on the template NCC

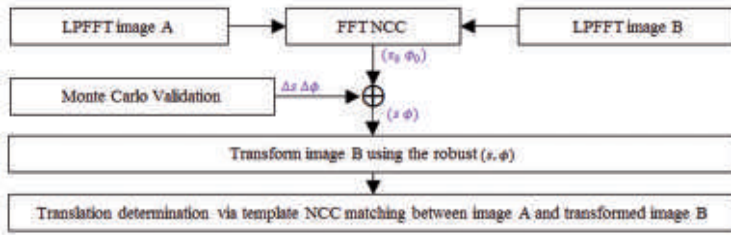


Fig. 5: Proposed similarity transform estimation method.

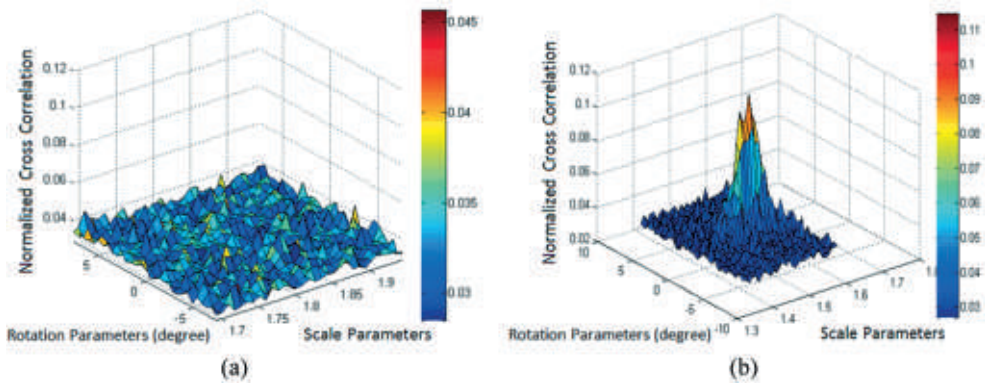


Fig. 6: (a) NCC value surface centred at wrong scale and rotation and (b) at correct scale and rotation.

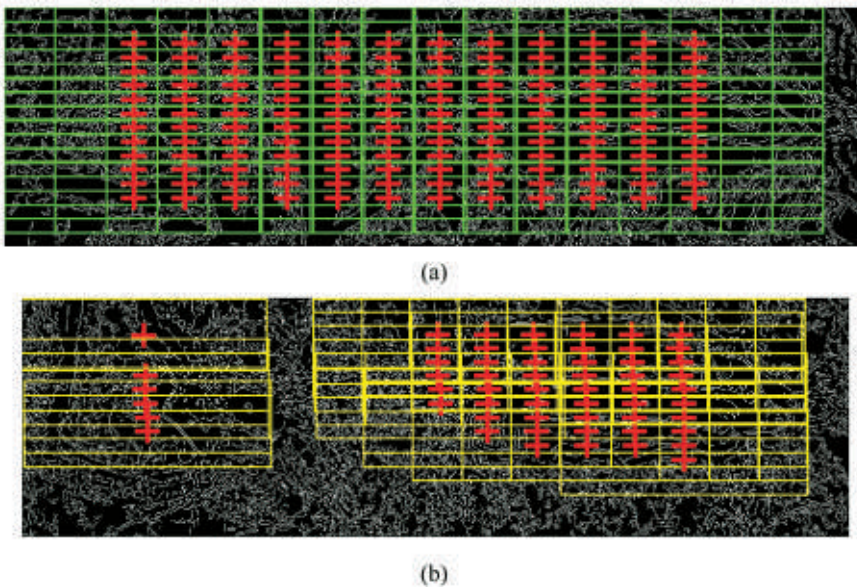


Fig. 7: (a) Reference patches in the LiDAR intensity edge image and (b) matched patches in the satellite edge image.

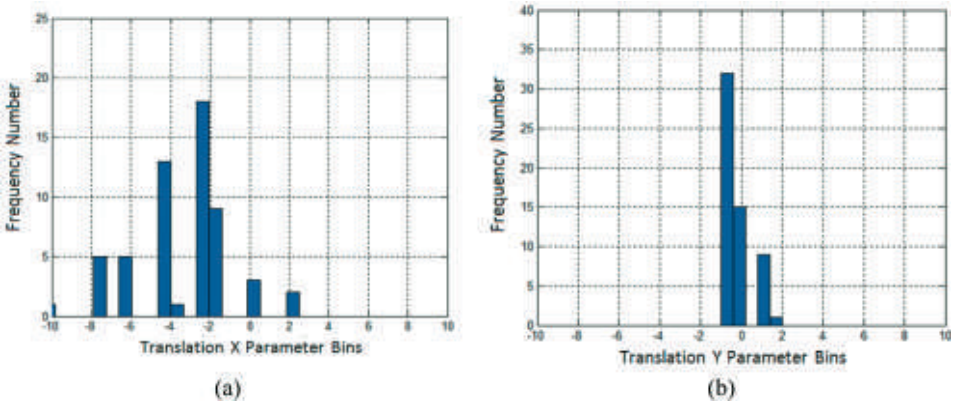


Fig. 8: (a) Histogram of column difference, translation in x and (b) row difference, translation in y.

matching. Fig. 7a shows the reference patches in the LiDAR intensity image A. Fig. 7b represents the matched templates in the second image. The template size is empirically determined, e.g. 0.3 times the image height and width. Ideally, image coordinate differences between all reference and matched patches should be identical. In reality, mismatches cannot be ruled out, and thus, the correct translation parameters are determined based on a statistical analysis of all column and row differences. For example, as shown in Fig. 8, most x-translations, t_x , fall between -3 and 0 pixels, and their accumulated total count over the interval is 28 out of 57. Similarly, the majority of y-translations t_y are between -1 and 0 pixels, totalling 47 out of 57. Thus, the average values $t_x = -2.5$, $t_y = -1$ pixels are accepted as the translation parameters.

3.2 Scale-, Rotation-invariant Regional PDF Descriptor Matching

The proposed feature generation and matching approach is illustrated in the Fig. 9. First, the HC detector is used to extract local feature points. As HCs in the two images are different, HCs from one image are transformed to the other image via the estimated similarity model from the adapted LPFFT. Square regions centred on those HCs are created in both images. Next, rotation-invariant kernel based PDF (probability density function) descriptor is created by applying a circular Epanechnikov kernel to the square region centred at the HC. The scale factor is known from the adapted LPFFT, hence the PDF descriptor is scale-invariant by adjusting the Epanechnikov

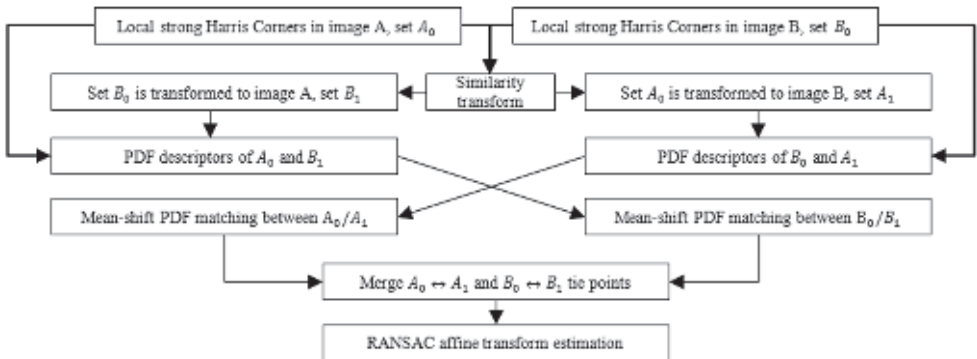


Fig. 9: Proposed affine transform estimation method.

kernel. The intensity PDF of the circular region is approximated by the normalized histogram; note for the 8-bit input image, the feature descriptor is 256-dimensional. Although the histogram is not the best nonparametric density estimation, it was proven to be sufficient for PDF matching purpose (COMANCIU et al. 2003). The similarity between two PDF descriptors is computed via the Bhattacharyya coefficient. Selecting PDF as feature descriptor is based on our earlier evaluation of multiple-domain image matching based on different feature spaces (Ju et al. 2011).

If the similarity transformation is adequate (and properly estimated), the transformed feature locations should be close to the correct positions, and consequently, PDF mean-shift matching can fast reach the local maximum. PDF mean-shift matching is an efficient and robust object tracking method which can track objects under different illumination conditions and perspectives. In short, it maximizes

the Bhattacharyya coefficient by finding the mode (peak) of the density in the local neighbourhood using mean-shift to recursively move to a new location (update). Feature region size can influence the PDF mean-shift matching performance and it is selected empirically. In our data, 50–110 pixels are appropriate. Fig. 10a shows an original feature in the LiDAR intensity image and Fig. 10b depicts the matched feature in the satellite image. Fig. 10c shows the PDF similarity score curve versus number of iterations; the local maximum is reached at the 4th iteration. Fig. 10d is the comparison between the reference PDF (blue) and the matched PDF (red).

All original features in the image pair are transformed to the other image; original features in the image A (set A_0) are transformed to the image B to form the set A_1 . The same operation is applied to the original features in the image B. The PDF mean-shift matching is performed on features between A_0 and A_1 as

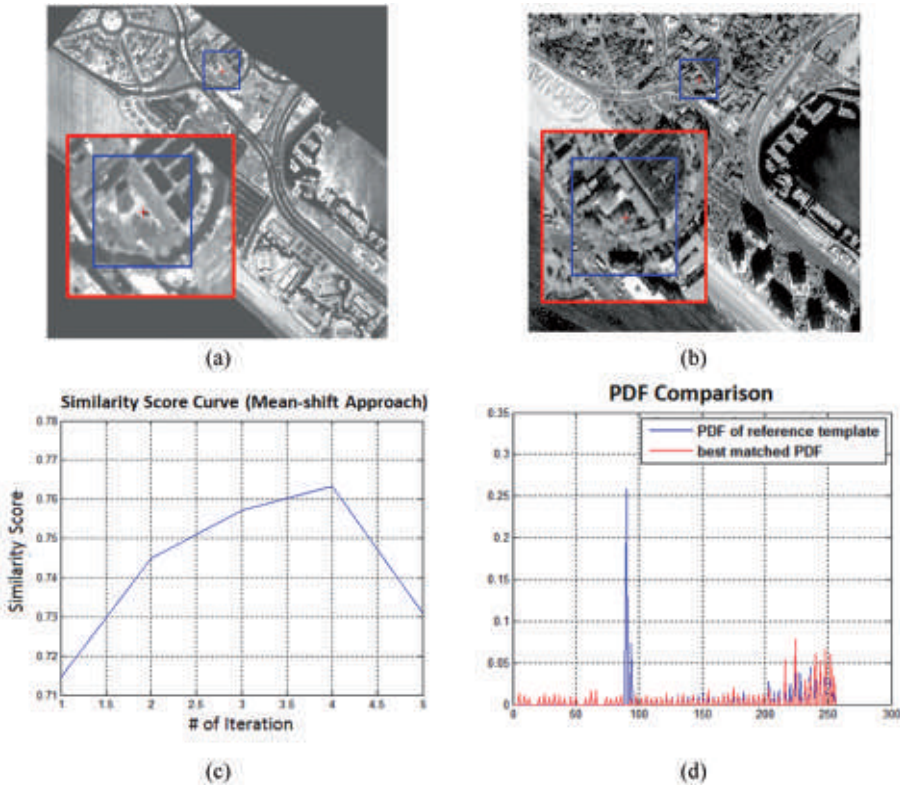


Fig. 10: (a) Feature location in the LiDAR intensity image, (b) matched feature location in the satellite image, (c) PDF similarity score curve and (d) comparison of reference PDF and matched PDF.

well as between B_0 and B_1 to find matched features with a similarity score larger than 0.7. Correspondences from $A_0 \leftrightarrow A_1$ and $B_0 \leftrightarrow B_1$ are merged as the complete set of tie points. Depending on object space characteristics, either affine and collinearity models, or more sophisticated models can be formed based on the matched feature locations. In all cases, blunder detection is necessary, which is based on RANSAC. In our test, RANSAC affine model estimation specifying a 0.5 pixel threshold for residual errors is used.

4 Experimental Results and Precision Analysis

The proposed approach was implemented in MATLAB and tested using the data introduced in section 1.4. Four aerial/LiDAR and satellite/LiDAR intensity image pairs were selected to evaluate the registration performance. The overlap is more than 90 % in the aerial/LiDAR and 100 % in the satellite/LiDAR image pairs. The extents of the overlap areas of the test image pairs are shown in Tab.1. After RANSAC affine model estimation, the number of inliers is more than enough to determine the 6 parameters of the affine transformation in all tests. The RMSE (root-mean-square error) of position errors is used to judge the registration precision. Similarly to the re-projection error, the position error is computed as the position difference between the matched and transformed points in the optical image. The RMSE is computed on

a pixel basis. As seen in Tab. 1, pixel level registration precision is obtained.

5 Conclusion

Feature-based SIFT registration, intensity-based MI registration, and frequency-based LPFFT registration methods were tested in this paper. Due to very different characteristics of LiDAR intensity and optical images, SIFT is unable to provide acceptable results based on our somewhat limited dataset. MI-based methods show good performance if the correct search range is given, which is a hard task. The traditional LPFFT has difficulty with finding the correct scale and rotation parameters from a set of candidates, and, in addition, the translation parameter determination is not reliable using FFT-accelerated NCC. Therefore, a hybrid method is proposed which is based on a two-step approach. The adapted LPFFT with a Monte Carlo validation check for the scale and rotation parameters, and estimating translation parameters based on the template NCC matching, is used to estimate an initial similarity transformation. Then, the scale- and rotation-invariant circular PDF descriptors centred at local strong HCs are created in each image, and then they are transformed to the other image via the estimated similarity transformation. The transformed feature location is the starting search position of a mean-shift PDF matching. In the final step, RANSAC affine model estimation is applied to the matched correspondences.

Tab. 1: Registration precision and performance and size of the test areas.

Aerial/LiDAR	3-11	3-12	4-11	4-12
Position RMSE (pixel)	0.95	1.16	0.99	1.13
Inlier/matched	16/30	11/25	8/16	15/26
Overlap size (m ²) Width(E) × Height(N)	463×811	465×804	473×823	458×818
Satellite/LiDAR	06	07	08	09
Position RMSE (pixel)	1.15	1.29	1.30	1.25
Inlier/matched	17/29	28/57	28/54	13/28
Overlap size (m ²) Width(E) × Height(N)	663×331	860×1426	723×970	326×575

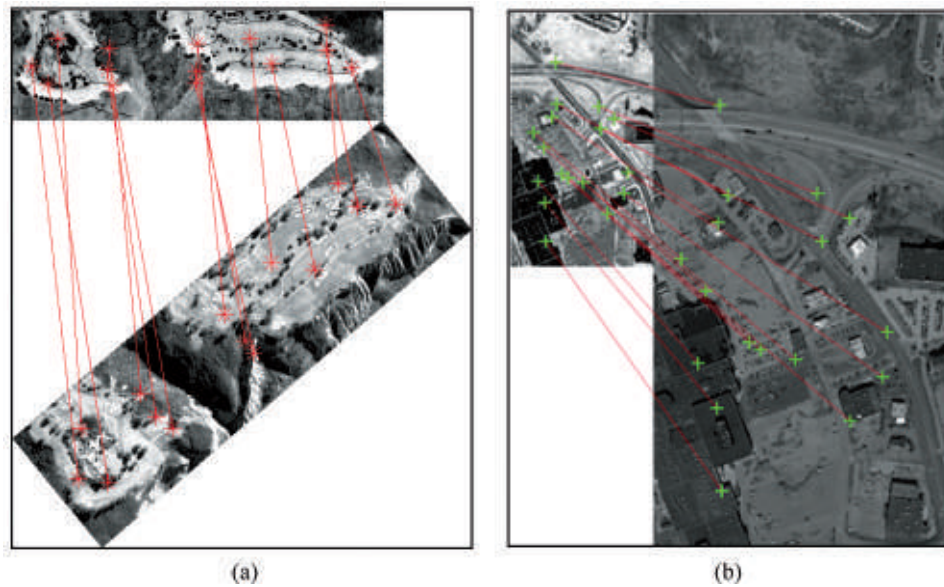


Fig. 11: (a) Registration between LiDAR intensity and satellite image pair, (b) between LiDAR intensity and aerial image pair.

This registration method is applied to LiDAR intensity and optical images. The results on a few image pairs have shown good performance, as pixel level registration precision was obtained.

Acknowledgements

The authors thank the GeoEye Foundation, Fugro-EarthData and ODOT for the data provided for this research.

References

- BECKER, S. & HAALA, N., 2008: Integrated LiDAR and Image Processing for the Modeling of Building Facades. – *PFG* **2008** (2): 65–81.
- BÖHM, J. & BECKER, S., 2007: Automatic Marker-Free Registration of Terrestrial Laser Scans using Reflectance Features. – *8th Conference on Optical 3D Measurement Techniques*: 338–344, Zürich, Switzerland.
- COMANICIU, D., RAMESH, V. & MEER, P., 2003: Kernel-based Object Tracking. – *IEEE Transactions on Pattern Analysis and Machine Intelligence* **25** (5): 564–577.
- FISCHLER, M.A. & BOLLES, R.C., 1981: Random Sample Consensus: A Paradigm for Model Fitting with Applications to Image Analysis and Automated Cartography. – *Communications of ACM* **24**: 381–395.
- GRÜN, A.W., 1985: Adaptive Least Squares Correlation: A Powerful Image Matching Technique. – *South African Journal of Photogrammetry, Remote Sensing and Cartography* **14**: 175–187.
- HABIB, A.F., GHANMA, M.S. & TAIT, M., 2004: Integration of LiDAR and Photogrammetry for Close Range Applications. – *International Archives of Photogrammetry, Remote Sensing and Spatial Information Sciences* **35** (B5).
- JU, H., TOTH, C.K. & GREJNER-BRZEZINSKA, D.A., 2011: Evaluation of Multiple-domain Imagery Matching based on Different Feature Spaces. – *2011 ASPRS Fall Conference*, Herndon, VA, USA, CD-ROM.
- KIM, C. & HABIB, A.F., 2009: Object-based Integration of Photogrammetric and LiDAR Data for Automated Generation of Complex Polyhedral Building Models. – *Sensors* **9** (7): 5679–5701.
- LIU, Z.Y., ZHOU, F.G., BAI, X.Z., WANG, H. & TAN, D.J., 2010: Multi-modal Image Registration by Mutual Information based on Optimal Region Selection. – *International Conference on Information, Network and Automation*: 249–253, Kunming, China.

- LOWE, D., 1999: Object Recognition from Local Scale-Invariant Features. – International Conference on Computer Vision: 1150–1157, Corfu, Greece.
- LOWE, D., 2004: Distinctive Image Feature from Scale-invariant Keypoints. – International Journal of Computer Vision **60** (2): 91–110.
- REDDY, B.S. & CHATTERJI, B.N., 1996: An FFT-based Technique for Translation, Rotation and Scale-Invariant Image Registration. – IEEE Transactions on Image Processing **5** (8): 1266–1271.
- REMONDINO, F. & RESSL, C., 2006: Overview and Experiences in Automated Markerless Image Orientation. – IAPRSSIS **36** (3): 248–254.
- SURI, S. & REINARTZ, P., 2010: Mutual Information Based Registration of TerraSAR-X and IKONOS Imagery in Urban Areas. – IEEE Transactions on Geoscience and Remote Sensing **48** (2): 939–949.
- TOTH, C.K., JU, H. & GREJNER-BRZEZINSKA, D.A., 2010: Experience with using SIFT for Multiple Image Domain Matching. – 2010 ASPRS Annual Conference, San Diego, CA, USA, CD-ROM.
- TOTH, C.K., JU, H. & GREJNER-BRZEZINSKA, D.A., 2011: Matching between Different Image Domains. – PIA 2011, Lecture Notes in Computer Science **6952**: 37–47, Munich, Germany.
- VIOLA, P. & WELLS, W.M., 1997: Alignment by Maximization of Mutual Information. – International Journal of Computer Vision **24** (3): 137–154.
- WOLBERG, G. & ZOKAI, S., 2000: Robust Image Registration using Log-Polar Transform. – 2000 International Conference on Image Processing **1**: 493–496.
- ZOKAI, S. & WOLBERG, G., 2005: Image Registration using Log-Polar Mapping for Recovery of Large-Scale Similarity and Projective Transform. – IEEE Transactions on Image Processing **14** (10): 1422–1434.

Address of the Authors:

Ph.D. candidate HUI JU, Dr. CHARLES TOTH, Prof. Dr. DOROTA A. GREJNER-BRZEZINSKA, The Ohio State University, Department of Civil, Environmental and Geodetic Engineering, 470 Hitchcock Hall, 2070 Neil Avenue, Columbus, OH 43213, USA, Tel.: +1-614-292-7681, Fax: +1-614-292-2957, e-mail: ju.32@osu.edu, toth@cfm.ohio-state.edu, dbrzezinska@osu.edu

Manuskript eingereicht: März 2012
Angenommen: Juni 2012